Journal of Chemical Health Risks

www.jchr.org

JCHR (2024) 14(1), 3198-3215 | ISSN:2251-6727

Therapeutic Potential of Hydrogel Based Sodium Alginate and Chitosan as A Multifunctional Drug Delivery System for Atopic Dermatitis

Kiran Singh[1], Mahendra Kumar Sahu[2], Deepa Thakur[3], Ume Kulsum[3], Lilima Baghel[4], Surabhi Sahu[5*], Jhakeshwar Prasad[6]

[1]Rungta College of Pharmaceutical Sciences and Research, Raipur – 492099, Chhattisgarh, India
[2]Kalinga University, Faculty of Pharmacy, Naya Raipur – 492001, Chhattisgarh, India
[3]Chhatrapati Shivaji Institute of Pharmacy, Durg – 491001, Chhattisgarh, India
[4]Shri Rawatpura Sarkar Institute of Pharmacy, Kumhari – 490023, Durg, Chhattisgarh, India
[5]RITEE College of Pharmacy, Chhatauna, Mandir Hasaud – 492101, Chhattisgarh, India
[6]Shri Shankaracharya College of Pharmaceutical Sciences, Junwani – 490020, Bhilai, Chhattisgarh, India

***Corresponding Author:** Surabhi Sahu
Email – sahusurabhi94@gmail.com

(Received: 25 December 2023 Revised: 10 January 2024 Accepted: 23 January 2024)

KEYWORDS
Hydrogel; Sodium alginate; Chitosan; Drug delivery system; Atopic dermatitis

ABSTRACT:
Tetramethylpyrazine (TMP) has low bioavailability due to its fast metabolism and short half-life, which is not conducive to transdermal treatment of atopic dermatitis (AD). Therefore, in this study, TMP was encapsulated into liposomes (Lip) by film dispersion method, and then the surface of Lip was modified by sodium alginate (ALG) and chitosan (CS). The tetramethylpyrazine-loaded liposomes in sodium alginate chitosan hydrogel called T-Lip-AC hydrogel. *In vitro* experiments, we found that T-Lip-AC hydrogel not only had the antibacterial effect of CS, but also enhanced the anti-inflammatory and antioxidant effects of TMP. In addition, T-Lip-AC hydrogel could also provide a moist healing environment for AD dry skin and produce better skin permeability, and can also achieve sustained drug release, which is conducive to the treatment of AD. The lesions induced by 1-chloro- 2, 4-dinitrobenzene were used as the AD lesions model to test the therapeutic effect of the T-Lip-AC hydrogel on AD *in vivo*. The studies have showed that T-Lip-AC hydrogel could effectively promote wound healing. Therefore, we have developed a T-Lip-AC hydrogel as multifunctional hydrogel drug delivery system, which could become an effective, safe and novel alternative treatment method for treating AD.

1. Introduction

Atopic dermatitis (AD), also known as atopic eczema, is a chronic inflammatory skin disease characterized by itchy, typically distributed eczema skin injury. Up to 20% of children and 10% of adults in the world suffer from AD. [1] AD is one of the most challenging skin diseases encountered by skin care professionals worldwide. Due to the decreased level of total ceramide in AD, it can damage the epidermal lipid tissue, and the abnormal differentiation of epidermal cell related molecules such as filaggrin can affect the hydration of the stratum corneum barrier, resulting in the dysfunction of the skin barrier function of AD. Some studies have shown that Th-1 cytokine in AD patients and Th-2 cytokine are usually over-expressed which is related to the chronic expansion of skin inflammation in AD. In addition, there are microorganisms on the skin surface, and the skin of AD patients is more susceptible to bacterial infection. About 90% of AD lesions are bacterial infection. [2] Therefore, by developing a safe and effective new drug preparation that can reduce AD inflammation, rebuild skin barrier and fight bacterial infection, this new drug preparation is expected to become an alternative treatment for AD. Tetramethylpyrazine (TMP) is a major active ingredient containing pyrazine ring found in traditional Chinese medicine that named *chuanxiong*. TMP has a variety of pharmacological activities, such as anticancer anti-kidney disease anti-thrombosis neuroprotection and so on. [3] In addition, it is reported that it has strong antioxidant and anti-inflammatory activities. Some studies have shown that TMP can not only clear reactive oxygen species (ROS) but also significantly inhibit the inflammatory factor IL-4,IL-

Journal of Chemical Health Risks

www.jchr.org

JCHR (2024) 14(1), 3198-3215 | ISSN:2251-6727

6,IL-13, TNF-α secreted by epidermal. [4] Consequently, TMP is a potentially effective drug for treating AD. Nevertheless, owing to its rapid metabolism, short half-life, the bioavailability of TMP is low, and its clinical application is limited. In recent decades, nanoparticle drug delivery systems have been recognized as a new type of drug delivery system due to their ability to prevent drug degradation, improve drug stability, enhance drug absorption, and improve drug bioavailability and tissue distribution. And these characteristics make it a very attractive drug delivery strategy. [5] Different types of nano carriers, such as polymer nanoparticles, solid lipid nanoparticles, and albumin nanoparticles, have been developed for various drug delivery applications. Therefore, contemporary research has proposed many different TMP packaging systems. Among them, Liposomes nanoparticles encapsulated with TMP has been proved to have high entrapment efficiency, improve the stability of TMP and prolong the action time of TMP. In addition, since Liposomes (Lip) is a lipid bilayer with amphiphilic properties, skin is essentially lipophilic. Therefore, Lipophilic properties of Lip allow it to rapidly penetrate across the stratum corneum to alleviate dermis. However, during storage, the structure of Lip is easily damaged by light, acid and alkali, resulting in problems such as flocculation, irregular drug release, etc. [6] In response, we have ultimately achieved an ideal drug release mode via the distribution *in vitro* and *in vivo* by changing the surface properties and composition of Lip. In recent years, it has been found that polyelectrolytes with opposite charges can self-assemble to form polyelectrolyte complexes (PEC) through electrostatic interactions. PEC surface coatings for Lip have many advantages, such as improving Lip stability, preventing drug leakage, prolonging its release, and increasing cell absorption of Lip. Therefore, PEC can bring substantial benefits to liposomes drug delivery systems. Sodium alginate (ALG) is a natural anionic polysaccharide derived from brown algae, which has good biocompatibility, biodegradability and adhesion. It is widely used as thickener, emulsifier and stabilizer in food, pharmaceutical and biomedical industries. [7] Chitosan (CS) is a cationic amino polysaccharide produced by deacetylation of chitin. Interestingly, due to the existence of amino group, CS dissolves in acidic solution and becomes cationic polysaccharide. In addition, CS also has unique characteristics such as polycationic properties, *in vivo* biodegradability, solubility in low pH aqueous media, mucosal adhesion, antibacterial activity, and wound healing, which have attracted widespread attention. Since the natural anionic polysaccharide ALG and cationic polysaccharide CS have opposite charges. Therefore, ALG can self-assemble with CS through electrostatic interaction to form PEC, thus forming a protective film on the surface of Lip, extending the retention time of drugs on the skin surface, and prolonging the drug action time. [8] At the same time, hydrogel is considered as an ideal wound dressing for skin because of its good flexibility and biocompatibility. It can create a humid environment conducive to tissue regeneration for the injured wound and avoid secondary injury caused by the adhesion of the injured wound, and facilitate the recovery of skin. This provides three-dimensional growth for skin cells, promotes interactions between biomolecules, cells, and tissues, thereby accelerating wound repair. In addition, CS has antibacterial activity which is essential to promote the treatment of AD. The multifunctional hydrogel with antibacterial, anti-inflammatory, antioxidant and skin healing properties were developed for the treatment of AD. For the treatment of AD, we have developed a multifunctional hydrogel drug delivery system that has the characteristics of anti-inflammatory, antibacterial, antioxidant, prolonging drug action time and promoting skin healing. In short, TMP was first coated in Lip by film dispersion method, and then T-Lip was put into ALG aqueous solution to prepare sodium alginate solution (T-Lip-A). [9] Finally, TMP-loaded Lip in sodium alginate and chitosan hydrogel (T-Lip-AC) to treat AD, which was formed by cross-linking T-Lip-A with the cross-linking solution prepared by mixing CS and CaCl2 (Fig. 1). In this experiment, we studied the physicochemical parameters of the preparation, such as viscosity parameters, entrapment efficiency, moisture absorption and delivery properties of the preparation, antibacterial ability, drug release, and antioxidant ability of the drug. In addition, the efficacy of T-Lip-AC was compared with TMP, T-Lip and T-AC in the animal model of AD induced by 1-chloro-2, 4-dinitrobenzene (DNCB) in mice, to explore the anti-inflammatory and antioxidant abilities of different preparations and their pharmacodynamic evaluation of the treatment of AD. [10]

2. Materials and Methods

2.1. Materials

TMP (purity 99%), phospholipids and cholesterol were purchased from Sigma-Aldrich, Mumbai (Maharashtra, India). ALG, sodium chloride solid, CS, Gelatin and 2-thiobarbituric acid (TBA) were purchased from Sigma-Aldrich, Mumbai (Maharashtra, India). Anhydrous calcium chloride was purchased from Sigma-Aldrich, Mumbai (Maharashtra, India). Acetic acid, sodium hydroxide solid, 1,1-diphenyl-2-picrylhydrazyl (DPPH) and FeSO4·7H2O were purchased from Loba Chemie Pvt. Ltd. Mumbai (Maharashtra, India). Anhydrous ethanol, acetone and trichloroacetic acid (TCA) were purchased from Loba Chemie Pvt. Ltd. Mumbai

Journal of Chemical Health Risks

www.jchr.org

JCHR (2024) 14(1), 3198-3215 | ISSN:2251-6727

(Maharashtra, India). Olive oil was purchased from Loba Chemie Pvt. Ltd. Mumbai (Maharashtra, India). DNCB was purchased from Sigma-Aldrich, Mumbai (Maharashtra, India). TSOD test kit was purchased from the Sigma-Aldrich, Mumbai (Maharashtra, India). The chemical reagents used in the experiment are analytically pure and do not need to be purified.

2.2. Animal

Healthy Kunming mice (male, 20 ± 2 g) were purchased from the Animal Experiment Center of Anhui University of Chinese Medicine (Hefei, China) and feed under constant environmental conditions (25 ± 2◦C, relative humidity 40-70%). These animals have free access to food and sterile water. All animal experiments comply with the guidelines approved by the Ethics Committee of Anhui University of Traditional Chinese Medicine (Hefei, China).

2.3. Determination of TMP standard curve

2.3.1. Determination of standard curve of TMP in vitro

Dissolve TMP powder in phosphate buffer solution (PBS, pH=7.4) to prepare TMP standard solutions of different concentrations. The absorbance was measured at 295 nm with an ultraviolet spectrophotometer. The standard curve of TMP in vitro was drawn with the mass concentration (C) of TMP as the abscissa and the absorbance (A) as the ordinate. Calculate the linear equation and correlation coefficient of the standard curve in vitro.

2.3.2. Determination of standard curve of TMP through mice skin in vivo

Shaved off the hair on the back of the blank mice, took the mice's back skin, and weighed it. Added 9 times the amount of 0.9% physiological saline according to the tare weight, and used a homogenizer to homogenize to obtain a skin homogenate suspension. Centrifuged at 6000rmp for 15min at low temperature, and took out the supernatant. PBS and five different concentrations of TMP solutions were added to the supernatant. The absorbance was measured at a wavelength of 295 nm using an ultraviolet spectrophotometer. The skin homogenate standard curve was drawn using the mass concentration (C) of TMP as the abscissa and the absorbance (A) as the ordinate. Calculate the linear equation and correlation coefficient of the standard curve of animal skin.

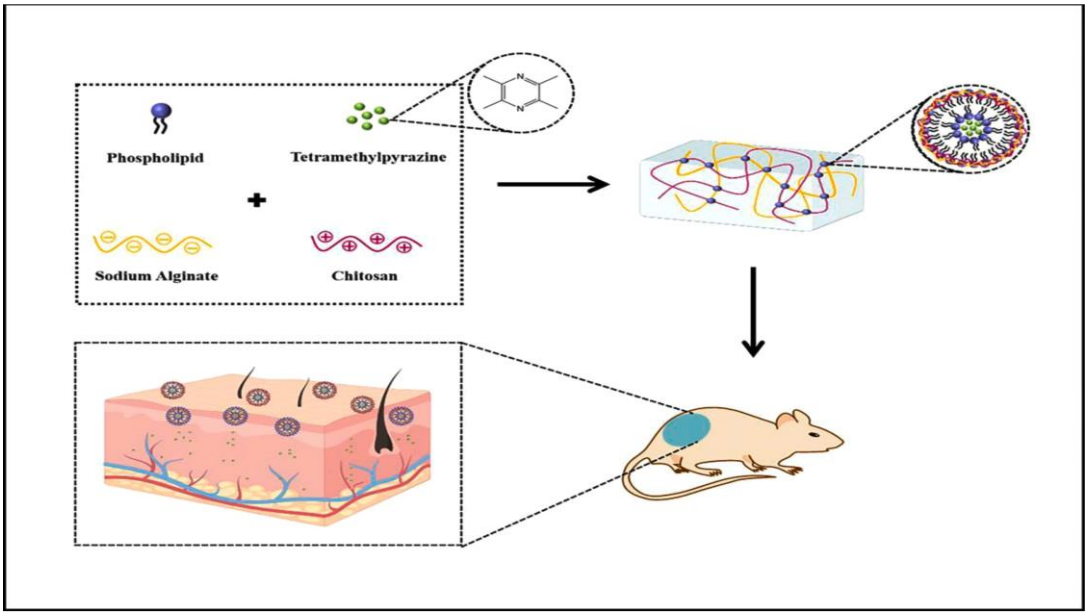

Fig.1. Preparation of tetramethylpyrazine-loaded liposomes surrounded by sodium alginate and chitosan hydrogel (T-Lip-AC) applied on the skin of AD-like mice.

2.4. Preparation and characterization of preparations

2.4.1. Preparation of TMP solution

Dissolve TMP powder in PBS (pH=7.4) to prepare a 0.6 mg/mL TMP solution. Store it in dark at 4 ◦C for future use.

2.4.2. Preparation of T-Lip

The liposomes were prepared using the thin film dispersion method developed by our laboratory. [11] In short, weigh soybean lecithin and cholesterol, add anhydrous ethanol, and dissolve them under ultrasound at 70 ◦C. The solvent was removed by rotary evaporation at 50◦C and a uniform transparent film was formed on the wall of round bottom flask. After that, a PBS solution containing TMP was added to a beaker

Journal of Chemical Health Risks

www.jchr.org

JCHR (2024) 14(1), 3198-3215 | ISSN:2251-6727

for hydration. Magnetic stirring was performed at 35◦C for 30 minutes, followed by ultrasonic treatment to

thoroughly mix Lip and TMP. Finally, PBS was used to dilute form T-Lip (0.6 mg/mL). Store the T-Lip suspension at 4◦C before use.

2.4.3. Preparation of T-AC and T-Lip-AC

The best ratio of CS and Ca2+ was determined by investigating the TAC viscosity of different ratios of CS and Ca2+. T-AC and T-Lip-AC were prepared with slight modification according to the existing preparation methods. [12] Take 4 mL of 1.5 mg/mL T-Lip suspension solution and add 0.1 g of ALG and 0.04387 g of NaCl solid, stirred it with a magnetic stirrer for 1 h, then to fix the volume to 5 mL using PBS, and continue stirring for 48 hours so that ALG could fully cover the surface of T-Lip, and adjust the pH to 7.0 with NaOH to make T-Lip-A (2 wt%, pH 8.0). Mixed CS (0.15 M NaCl aqueous solution 1.5 wt%, pH 6.0) and CaCl2 (50 mM aqueous solution, pH 8.0) to form a crosslinker solution according to different volume ratios. Finally, T-Lip-AC hydrogel was formed by mixing T-Lip-A with equal volume cross-linking agent solution (mixed solution of CS and CaCl2). Change T-Lip suspension into TMP solution, and use the same steps to prepare T-AC hydrogel.

2.4.4. Viscosity measurement

The viscosity was measured by Ubbelohde capillary viscometer. [13] Mix the formulation with PBS in a volume ratio of 1:9 at room temperature. After mixing, measure with a capillary viscometer, recorded the time. Calculated the viscosity of the hydrogel (η2) using formula (1).

$\eta 2 = \rho 2t2$

$\rho 1t1 * \eta 1$ (1)

In the formula, "η" Is the viscosity (mpa · s), "ρ" Is the density (g/mL), and "t" is the time (s); "1" represents PBS, and "2" represents sample.

2.4.5. Observation of Appearance, Determination of Zeta Potential, Particle Size, morphology and pH Value

The prepared gel was visually tested for color and clarity. The Zeta potential and particle size of T-Lip and T-Lip-AC were measured by particle size analyzer. Observe the morphology of Lip in T-Lip under a transmission electron microscope using existing method. [14] At the same time, use a pH meter to measure the pH value of different preparations.

2.4.6. Entrapment efficiency

In order to separate the unembedded drugs from formulation, the entanglement efficiency was measured. Mix the formulation with PBS in a volume ratio of 1:4, and centrifuged at the speed of 13000 rpm for 1 h. collected the supernatant, the absorbance of free TMP in the preparation was measured using an ultraviolet spectrophotometer at a wavelength of 295 nm, and the drug concentration of free TMP in the preparation was calculated based on the linear equation of the TMP *in vitro* standard curve. Then dilute the formulation with ethanol mixture, dissolve the liposome membrane with ultrasound, and centrifuged at 13,000 rpm for 1h. Then the supernatant is filtered by using 0.22 μm milli-pore membrane, the filtered supernatant was collected, the absorbance of free TMP in the preparation was measured using an ultraviolet spectrophotometer at a wavelength of 295 nm, and the drug concentration of total TMP was calculated according to the linear equation of the TMP *in vitro* standard curve. Use formula (2) to calculate the entrapment efficiency (%).

Entrapment Efficiency (%) = (Wt - W*f*)

W*t* × 100% (2)

In the formula, "W*t*" represents the total TMP drug content (mg), and "W*f*" represents the free TMP drug content (mg).

2.5. Determination of hygroscopicity of T-Lip-AC hydrogel

In order to measure the hygroscopicity of T-Lip-AC hydrogel, the weight of the formulation after hygroscopic treatment was compared with that before hygroscopic treatment. Calculate the hygroscopicity of the hydrogel using formula (3).

Hygroscopicity of Hydrogels per unit Weight = (W1 - W0)

W1 × 100% (3)

In the formula, "W1" represents the mass of the sample after moisture absorption (g), and "W0" represents the mass of the sample before moisture absorption (g).

2.6. Determination of moisture feeding performance of T-Lip-AC hydrogel

Simulate skin with gelatin, apply the T-Lip-AC hydrogel onto the gelatin, and seal with cling film and sealing film. After 48 hours, take out the hydrogel from the gelatin, and measure the moisture feeding performance of T-Lip-AC hydrogel by calculating the weight difference of the formulation before and after the formulation measurement.

2.7. Drug release study: The transmembrane and transdermal release Experiments

According to the method previously reported we used the dialysis membranes and isolated back skin tissue from normal mice to evaluate the transmembrane and transdermal ability of different preparations. [15] The Franz diffusion cell was used to study the drug release. In short, the dialysis membrane/normal mice back skin was placed between the donor and receiver cell of the

Journal of Chemical Health Risks

www.jchr.org

JCHR (2024) 14(1), 3198-3215 | ISSN:2251-6727

Franz diffusion well, and a release medium (PBS, PH 7.4) was added to the receiver cell. Then, added 1.0 mL TMP, T-Lip, T-AC, T-Lip-AC (equivalent to 0.6 mg TMP) into the donor compartment and seal both ends of the diffusion well. At 0.125, 0.25, 0.375, 0.5, 1, 2, 3, 4, 5, 6, 7, 8, 9, 10, 11, 12, 24, 36, 48, 60, 72, 84, 96 h, 2 mL of sample solution was extracted from the receiver cell, and 2 mL of release medium was added to maintain the conditions of the receptor compartment. Measure the absorbance of the sample solution at 295 nm using an ultraviolet spectrophotometer, and bring the measured absorbance values into the standard curve linear equations to calculate the concentration of "Cn". The cumulative drug release rate was calculated by formula (4). Finally, the release of different preparations *in vitro* and *in vivo* was evaluated by fitting data in Weibull CDF model and comparing R2.

Cumulative Drug Release (%) = $Cn * Vn + \sum n\ i=-\ 11 Ci * Vi$
$Qt * 100\%$ (4)

In the formula, "*Cn*" is the drug concentration of the dissolution medium at each sampling time point; "*Ci*"is the drug concentration in the sample; "*Vn*" and "*Vi*" are the volume of dissolved medium and sample respectively; "*Qt*" is the theoretical dose.

2.8. Study on antibacterial capacity in vitro

Conduct in vitro antibacterial capacity studies on T-Lip, T-AC, and TLip-AC by observing changes in the appearance, pH, entrapment efficiency, and viscosity of the formulation. All formulations are stored in dark conditions at 25◦C and regularly observed every 5 days.

2.9. Study on antioxidant capacity in vitro

DPPH clearance test: The experiment was divided into blank control group, sample group, and sample control group. The blank control group consisted of absolute ethanol and 0.08 mg/mL DPPH absolute ethanol solution, the sample group consisted of TMP preparation and 0.08 mg/ mL DPPH absolute ethanol solution, and the sample control group consisted of TMP preparation and absolute ethanol solution. Evenly mix and incubate under 37◦C in dark for 30 min. After that, the absorbance of each solution was measured at 517 nm using an ultraviolet spectrophotometer. Use formula (5) to calculate the scavenging rate on DPPH (%). H2O2 removal test: The experiment was divided into blank control group, sample group, and sample control group. The blank control group was composed of PBS and 40 mmol/mL H2O2 solution, the sample group was composed of sample and 40 mmol/mL H2O2 solution, and the sample control group was composed of sample and PBS. Evenly mix and incubate under 37◦C in dark for 10 min. After that, the absorbance of each solution was measured at 230 nm using an ultraviolet spectrophotometer. Use formula (5) to calculate the scavenging rate on H2O2 (%).

Scavenging Rate (%) = $Ao - (As - Ac)\ A\ o * 100\%$ (5)

In the formula, "*Ao*" represents the absorbance of the blank control group, "*As*" represents the absorbance of the sample group, and "*Ac*" represents the absorbance of the sample control group.

2.10. Building the animal AD model

In order to establish AD model in mice, DNCB was applied locally on the back skin of mice to induce specific dermatitis. The mice were randomly divided into group B, group M, group P and preparation group. Shave off their back hair the day before the experiment, and use DNCB 5%, dissolved in acetone and olive oil 3:1 (v/v)] sensitized group M, group P and preparation group containing TMP. The same volume of acetone: olive oil = 3:1 (v/v) was used in the group B for 2 days. From the 4th day, group B and group M were smeared with PBS, group P was treated with dexamethasone cream (DXMS), and the preparation group was smeared with TMP, T-Lip, T-AC, T-Lip-AC on the back for 13 days. The dose of TMP used in all preparation groups was same dose each time, once a day. All mice were killed and sampled on the 17th day. Photographs of mice back skin were taken on days 0, 3, 7, 12 and 16. AD score was divided into 5 items (erythema, edema/papule, peeling/scratch, exudation/scab, lichenization) according to the skin lesions. The severity of each skin lesion was scored on a scale of 0 to 3 points. 0 points is zero (that is, the physical sign cannot be determined after careful observation), 1 point is light (that is, the physical sign does exist, but can be seen only after careful observation), 2 points is medium (that is, the physical sign can be seen immediately), 3 points is heavy (that is, the physical sign is very obvious). The score between various symptoms can be recorded as 0.5 points.

2.11. Evaluation of the antipruritic effect of T-Lip-AC

To test the antipruritic effect, the number of scratches on the back skin of mice was evaluated. On the 16th day, the scratching behavior of mice was recorded within 20 min. The mice raised its paw and scratched it continuously for a long time, until the paw returned to the floor, which was recorded as a scratch.

2.12. Histopathological analysis of skin tissue

In order to further study the treatment of AD, the mice back skin tissue was collected and fixed with 4% paraformaldehyde solution. Skin sections with appropriate thickness were prepared and stained with hematoxylin and eosin (H&E) for histopathological analysis.

Journal of Chemical Health Risks

www.jchr.org

JCHR (2024) 14(1), 3198-3215 | ISSN:2251-6727

2.13. Spleen index

To study the changes of spleen index in AD animals. The spleen tissue of mice was isolated, weighed. Use formula (6) to calculate the spleen index. Spleen Index = Spleen mass (mg) / Body mass (g) (6)

2.14. Evaluate the effect of T-Lip-AC hydrogel on the activity level of malondialdehyde (MDA)

Remove the mice's back skin, heart, liver, lungs, kidneys, and brain tissue. Wash, dry, and weigh. According to the weighed tissue weight, add 0.9% cold physiological saline at a specific gravity of 1:9, and use a homogenizer to grind the homogenate. Centrifuge at 4000 rpm for 15 min and take the supernatant. The experiment was divided into blank group, model group, and sample group. Take supernatant, add normal saline to the blank and model groups, and add sample to the sample group. Let stand for 5 min. Add 5.6% TCA solution to each group and let stand for 5 min. Then add 0.375% TBA solution. Mix well and take a 95◦C water bath for 40 min. Cool, centrifuge at 4000 rpm for 8 min, and take the supernatant. At 532 nm, zero the solution with normal saline, and then measure the absorbance of each solution. The inhibition rate (%) of MDA generated by TMP, T-Lip, T-AC, T-Lip-AC on skin and heart, liver, lung, kidney and brain tissues were calculated by formula. [16]

MDA Inhibition Rate(%) = Am – As

Am - As ∗ 100%

Where, "*Am*" is the absorbance value of the model group; "*As*" is the absorbance value of the sample group; "*Ab*" is the absorbance value of the blank group.

2.15. Evaluate the effect of T-Lip-AC on superoxide dismutase (SOD) activity

Take the skin from the animal's back, wash it, dry it, and weigh it. According to the weight, 0.9% cold physiological saline was added at a specific gravity of 1:9, and homogenization was performed using a homogenizer to obtain a skin homogenate suspension. 6000 rpm centrifugation for 15 min, taking supernatant, add different application solutions in sequence according to the steps of the SOD kit, and mix. Take a constant temperature water bath at 37◦C for 40 min, and add developer. Mix and place at room temperature for 10 min. The absorbance was measured at a wavelength of 550 nm.

2.16. Determination of TMP content in skin of AD mice

The back skin of mice in the TMP preparation group was taken and weighed. Add 9 times the amount of 0.9% physiological saline according to the weight, and use a homogenizer to homogenize to obtain a skin homogenate suspension. Centrifuge at 6000 rpm for 15 min at low temperature, and take the supernatant. The absorbance was measured at a wavelength of 295 nm using an ultraviolet spectrophotometer. Bring it into the linear equation of the mice skin standard curve to calculate the drug content.

2.17. Statistical analysis

All data are expressed as mean ± standard deviation (SD), N ≥ 3. SPSS 25.0 was used for statistical analysis, and one-way ANOVA tests were employed to show statistical differences between groups, *p <0.05 was considered statistically significant.

3. Results

3.1. TMP standard curve

The standard curve was drawn with the mass concentration (C) of TMP as the abscissa and the absorbance (A) as the ordinate. The standard curve of TMP *in vitro*: A = 0.0365∗C + 0.0273 (R2 = 0.9991); The standard curve of TMP through mice skin *in vivo*: A = 0.018∗C + 0.4079 (R2 = 0.9945). The two linear regression equations R2 are both greater than 0.99, indicating a good linear relationship between TMP drug concentration and absorbance within this concentration range.

3.2. The T-Lip-AC formulation study

Different from solutions, hydrogels need to have certain mechanical properties. It is reported that when the concentration of ALG is constant, CS and Ca2+ will affect the mechanical properties of the hydrogel. [17] Therefore, in order to obtain the most suitable hydrogel for the skin surface of mice with AD symptoms, we determined the optimal ratio by investigating the viscosity of hydrogels containing CS and Ca2+ in different proportions when the ALG concentration was constant. Preliminary screening found that when the volume ratio of CS:Ca2+ = 1:1, the viscosity of T-AC was the largest (3.43 ± 0.072 mPa· S), and can maintain a semi solid state (Fig. 2 and Table 1). After that, the viscosity decreased with the increase of Ca2+ concentration, flocculent coagulation and agglomeration occurred at CS: Ca2+ = 1:4 (v/v) and CS: Ca2+ = 0:1 (v/v). After the addition of Lip, the viscosity of T-Lip-AC with the same CS and Ca2+ratio significantly increased, and the trend of change was consistent with that of T-AC. At the same time, flocculent coagulation and agglomeration phenomenon also began to occur in CS: Ca2+ = 1:4 (v/v) and CS: Ca2+ = 0:1 (v/v), and the phenomenon was more obvious (Table 1). Therefore, we decided to finally choose the ratio of CS: Ca2+ = 1:1 (v/v) to prepare T-AC and T-Lip-AC hydrogels.

Journal of Chemical Health Risks

www.jchr.org

JCHR (2024) 14(1), 3198-3215 | ISSN:2251-6727

Table 1. Viscosity of T-AC and T-Lip-AC with different proportions of CS and Ca2+.

Proportion of CS and Ca2+	Viscosity of T-AC (mPa·S)	Viscosity of T-Lip-AC (mPa·S)
CS: Ca2+ = 4:1	2.33 ± 0.019	13.72 ± 0.192
CS: Ca2+ = 3:2	2.51 ± 0.038	14.23 ± 0.157
CS: Ca2+ = 1:1	3.43 ± 0.072	18.82 ± 0.186
CS: Ca2+ = 2:3	2.56 ± 0.002	13.94 ± 0.127
CS: Ca2+ = 1:4	2.38 ± 0.166	6.19 ± 0.085
CS: Ca2+ = 0:1	2.16 ± 0.014	5.26 ± 0.036

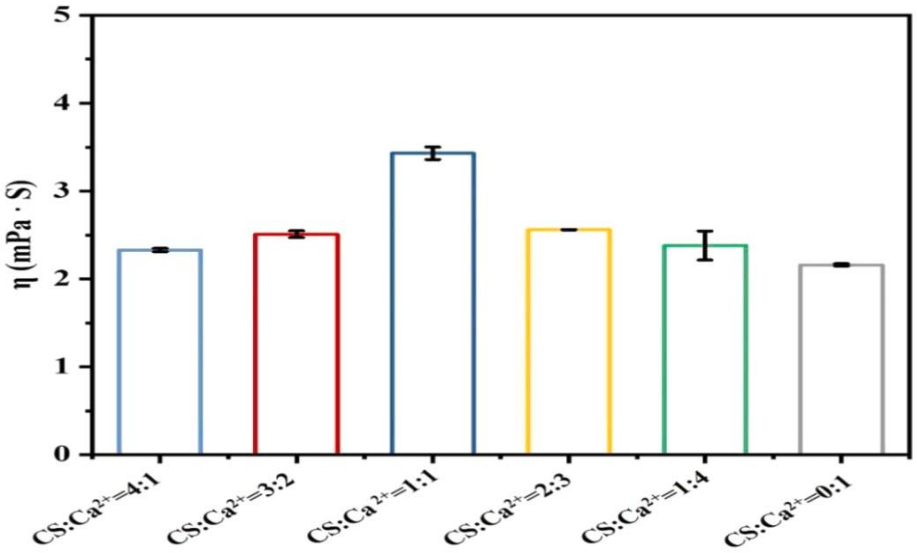

Fig. 2. Viscosity of T-AC with different proportions of CS and Ca2+.

3.3. Morphological characteristics and physical properties of TMP-loaded preparations

T-Lip was light yellow suspension solution, and the distribution was uniform, the zeta potential of T-Lip was - 24.2 ± 3.7 mV, and it appears spherical under transmission electron microscope, with an average particle size of 126 ± 12.55 nm. The appearance of optimized T-Lip-AC hydrogel was light yellow, uniform distribution, and without flocculent condensation. The zeta potential of T-Lip-AC was - 7.45 ± 0.28 mV, the average particle size was 285 ± 19.38 nm. In addition, the pH value of TLip-AC was 6.93 ± 0.12, which had no irritating effect on mice skin. The entrapment efficiency of T-Lip was determined by ultraviolet spectrophotometry. The same operation was performed on the blank liposome and the absorbance at 295 nm was determined. The results showed that the absorbance of blank liposomes could be ignored. It showed that the lipid and other components in the liposomes were not absorbed at 295 nm and would not interfere with the absorbance of the drug. The entrapment efficiency of T-Lip was 62.15 ± 3.59%, that of T-AC was 68.36 ± 4.7%, and that of T-Lip-AC was 74.8 ± 2.4%.

3.4. Test of hygroscopicity and moisture supply performance of T-Lip-AC hydrogel

The hydrogel with good hygroscopicity can effectively reduce the accumulation of wound exudate, and keep the wound in a moderately wet environment. [18] Therefore, the hygroscopicity of hydrogel is one of the indicators to evaluate the performance of hydrogel. It can be seen from Table 2 that under the condition of the same ALG concentration, changing the amount of CS and Ca2+ had no significant impact on the hygroscopicity of the hydrogel. The hygroscopicity of T-AC hydrogel prepared under different ratio conditions was mostly about 0.8 times of its own mass. The addition of Lip had little impact on the moisture absorption ability of the preparation. The moisture supply performance of hydrogel is also an important index to evaluate the performance of hydrogel. In the experiment, 35 % gelatin was selected to simulate dry skin wounds. In the experiment, the water gel was contacted gelatin, and the water lost by the gel was the water absorbed by gelatin, which usually represented the ability of the gel to give a wet environment to dry wounds. [19] We found that before the T-Lip-AC experiment, there was 5.65 g, and after contact with gelatin, the weight was 4.62 g, losing 18.2% of water. Therefore, T-Lip-AC hydrogel has good moisture

Journal of Chemical Health Risks

www.jchr.org

JCHR (2024) 14(1), 3198-3215 | ISSN:2251-6727

transfer performance. Because T-Lip-AC hydrogel could deliver a certain amount of water to dry skin, and it could also have certain hygroscopicity when the wound exudate increased, which are conducive to the recovery of AD lesion skin. [20]

3.5. Drug release study: The transmembrane and transdermal release experiments

PBS solution with pH 7.4 was selected as the diffusion medium in the lower chamber, and the dialysis membrane and normal mice skin were used to simulate the local release of drugs under the physiological environment *in vitro* and *in vivo*. The cumulative release percentage of TMP, T-Lip, T-AC and T-Lip-AC at each time point was shown in Fig. 3. In the drug transmembrane release experiment across dialysis membrane (Fig. 3A), about 40.04 ± 3.24% of TMP was released from TLip within 11 h, and about 61.07 ± 4.73% from T-Lip-AC within 24 h. Compared with T-Lip, T-Lip-AC reached its peak more slowly, but the drug release rate increased significantly. In the drug transdermal release experiment across isolated skin (Fig. 3B), T-Lip-AC not only accelerated drug release compared to the TMP release curve, but it also demonstrated the function of drug storage and enhanced the ability of drugs to penetrate the skin. The drug release curve was analyzed with Weibull CDF model (Table 3). In the drug transmembrane release experiment across dialysis membrane, the R2 value of T-Lip-AC was 0.98170. In the drug transdermal release experiment across isolated skin, the R2 value of T-Lip-AC was 0.97498. There showed that the Weibull CDF model was suitable for the *in vitro* and *in vivo* release of T-Lip-AC hydrogel, which was feasible and had a linear relationship. Overall, T-Lip-AC provides TMP with good drug release and enhanced drug penetration through the skin, which may be beneficial for the treatment of AD.

3.6. Study on antibacterial capacity in vitro

In order to verify that the addition of CS could indeed make T-Lip-AC hydrogel antibacterial, the preliminary antibacterial performance test was carried out for the newly prepared T-Lip-AC hydrogel, which was stored at 25◦C in the dark to observe the bacterial growth. We found that bacteria appeared on the surface of T-Lip around the 5th day, bacteria appeared on the surface of T-Lip-AC around the 10th day, and bacteria appeared on the surface of T-AC around the 15th day. So, adding CS has a certain antibacterial effect (Table 4).

3.7. Study on antioxidant capacity in vitro

In order to measure the antioxidant capacity of TMP, we first conducted an *in vitro* antioxidant capacity test. It was shown in Fig. 4A and 4B the scavenging rate of TMP solution with different concentrations (0.2, 0.4, 0.6, 0.8, 1.0 and 1.5 mg/mL) on DPPH and H2O2. It was found that scattering rate of TMP solution was concentration dependent on H2O2 and DPPH radial. Within the concentration range of 0.2~0.6 mg/mL TMP, the scavenging rate of TMP on H2O2 and DPPH increased with the increase of concentration. After that, with the increase of TMP concentration, there is little change in H2O2 and DPPH radial scanning rate. At a concentration of 0.6 mg/mL, TMP achieved 70.62 ± 4.06% and 71.76 ± 3.86% scavenging rate on H2O2 and DPPH at 2 h, indicating that TMP had strong antioxidant activity. In order to further determine the antioxidant activity of TMP-loaded preparations and the effect of excipients on its antioxidant performance. the scavenging ability of TMP solution, T-Lip, T-AC and T-Lip-AC to free radicals were determined and compared. The results in Fig. 4C and Fig. 4D were shown that T-Lip, T-AC and T-Lip-AC had strong antioxidant activity against H2O2 and DPPH at 2 h, which had a greater than 60% of the anti-oxidative capacity. The results in Fig. 4C and 4D proved that TMP maintained its antioxidant properties after encapsulation, indicating that the encapsulation conditions had no significant impact on the antioxidant activity of TMP. Therefore, in the presence of T-LipAC, TMP became more stable than free TMP solution, and would not have a meaningful impact on its antioxidant activity, thus expanding its application in antioxidant.

Journal of Chemical Health Risks

www.jchr.org

JCHR (2024) 14(1), 3198-3215 | ISSN:2251-6727

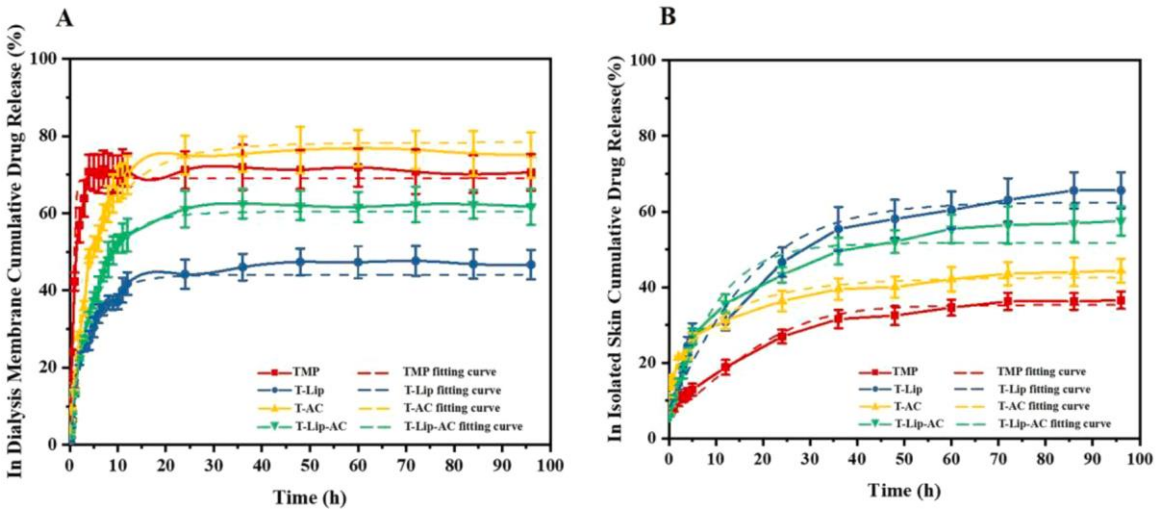

Fig.3. Drug release studies of TMP, T-Lip, T-AC and T-Lip-AC *in vitro* and *in vivo*. (**A**) Drug transmembrane release experiment across the dialysis membrane; (**B**) Drug transdermal release experiment across isolated skin.

3.8. T-Lip-AC alleviates AD-like symptoms in DNCB-induced in mice skin

In order to evaluate the therapeutic effect of T-Lip-AC on AD, we applied dexamethasone cream (DXMS), TMP, T-Lip, T-AC, T-Lip-AC to the DNCB-induced AD mice pathological model. The AD model was established by applying DNCB to the skin, and then the mice were given therapeutic drugs on the 4th day (Fig.

5A). On the 17th day, the healing effect was evaluated by animal skin pictures and histological examination. According to the general picture observation (Fig. 5B), Mice in model group (group M) showed severe skin inflammation, swelling, sparse hair and red skin. DNCB induction followed by T-Lip-AC showed significant improvement in skin inflammation; The result was almost the same as that of blank group (group B) mice. The appearance of skin healing in mice were observed and evaluated. After DNCB induction, the animals that only received PBS treatment (group M) average scored 3, indicating almost no healing. The average healing level of animals treated with TMP was 2, and the average healing level of animals treated with T-Lip and T-AC was 1. The average healing grade of positive control group (group P) receiving DXMS treatment and T-Lip-AC treatment was 0.5. In addition, it was found that after the treatment of T-Lip-AC, the number of scratches was significantly reduced compared with that of group M, which was close to that of group P (Fig. 5C). Therefore, T-LipAC might have the effect of relieving AD symptoms induced by DNCB. Surprisingly, we found that group P mice treated with DXMS began to experience slow skin recovery, significant weight loss, and even death on 7th day. Moreover, the skin of mice in group P was drier than that in T-Lip-AC group. These problems might be due to DXMS being a glucocorticoid drug and adverse reactions in mice. Thus, it is necessary for us to find more effective alternatives.

Journal of Chemical Health Risks

www.jchr.org

JCHR (2024) 14(1), 3198-3215 | ISSN:2251-6727

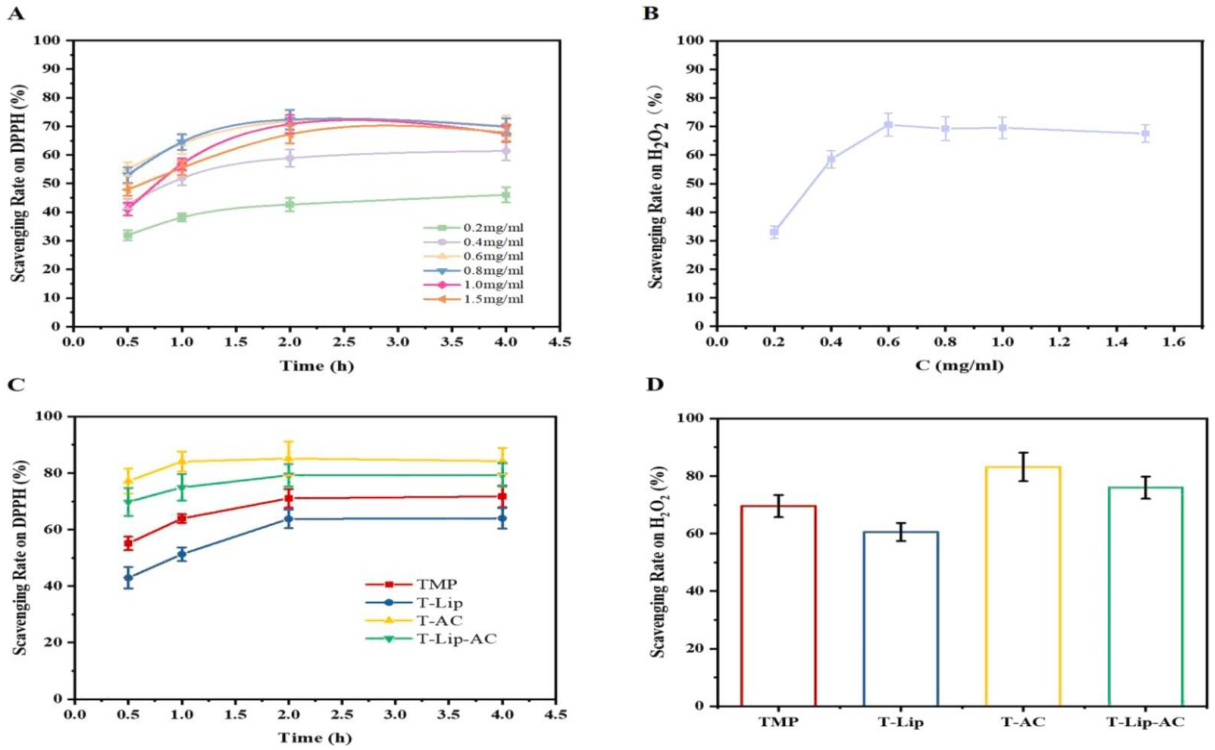

Fig.4. Study on antioxidant capacity *in vitro*. (**A**) The scavenging rate of TMP solution with different concentrations on DPPH; (**B**)The scavenging rate of TMP solution with different concentrations on H2O2; (**C**)The scavenging rate of TMP with different dosage forms of 0.6 mg/mL on DPPH; (**D**)The scavenging rate of TMP with different dosage forms of 0.6 mg/mL on H2O2.

3.9. T-Lip-AC decreased epidermal thickness and mast cell infiltration in mice with DNCB-induced AD-like skin lesions

In order to observe the overall inflammation, the skin of mice was stained with hematoxylin and eosin (H&E). DNCB-induced AD in group M, H&E staining showed obvious epidermal tissue proliferation, epidermal cell hypertrophy, and severe inflammatory cells infiltrating the dermis, indicating the occurrence of AD-like disease. [21] It was worth noting that the group receiving T-AC showed slight hypertrophy of the epidermis, with few inflammatory cells infiltrating the dermis, similar to that of group P. This might be because CS had antibacterial activity and ALG-CS hydrogel was conducive to wound recovery. In the histomorphology analysis of tissue sections, T-Lip-AC group showed a slightly hypertrophic epidermis and no inflammatory cells infiltrating the dermis, which confirmed the excellent healing observed in the gross picture (Fig. 6).

3.10. T-Lip-AC hydrogel reduces inflammatory response in AD-like mice

The spleen is one of the most important immune and lymphatic organs in the human body, which can increase during inflammatory reactions. [22] Therefore, it plays an indicative role in the strength of human immune function. To further examine the recovery of DNCB induced skin inflammation, we compared the spleen index of mice. It was shown in Fig. 7 that the use of DNCB resulted in a significant increase in the spleen index in mice, indicating that splenomegaly was caused by inflammatory symptoms of AD compared to group B animals. We found that the spleen index of TMP-loading preparations was generally lower than that of group P. And the spleen index of T-Lip-AC was significantly lower than that of other preparations (3470 ± 183.66 mg/g) and close to that of group B (3479 ± 250.49 mg/g). This indicated that T-Lip-AC had a higher anti-inflammatory effect and had a better therapeutic effect on the remission of AD symptoms. [23]

3.11. Evaluate the effect of T-Lip-AC on MDA activity

The effect of different TMP preparations on the MDA activity levels of different organs is shown in Fig. 8, it was found that the inhibition rate on MDA in the skin and organs of mice treated with T-Lip-AC was higher than that of other preparations. In addition, we found that the inhibition rate of TMP on cardiac MDA was not as high as that of the group P, which might be due

Journal of Chemical Health Risks

www.jchr.org

JCHR (2024) 14(1), 3198-3215 | ISSN:2251-6727

to the low sensitivity of TMP to the heart. In general, the high inhibition rate of T-Lip-AC indicated that it reduced the level of lipid peroxidation *in vivo*, and its antioxidant effect was better than other preparations, which was helpful for the treatment of AD.

3.12. Evaluate the effect of T-Lip-AC on SOD activity

It was found in Fig. 9 that the SOD value of group M (2505.12 ± 943.92 U/mg · prot) was significantly lower than that of group B (4661.37 ± 340.02 U/mg · prot). Compared with TMP (2848.53 ± 462.67 U/mg · prot), T-Lip (3188.36 ± 516.59 U/mg · prot) and T-AC (3470.79 ± 344.42 U/mg · prot), it was observed that the level of SOD activity (4117.12 ± 378.4 U/mg · prot) after treatment with T-Lip-AC was significantly higher, and close to the value of group B, which indicated that T-Lip-AC could reduce AD oxidative stress caused by decreased antioxidant levels in the body.

3.13. Study on the content of TMP in the skin of AD-like mice

In order to detect the drug content in AD–like mice skin, the absorbance of mice skin in the preparation group was brought into the pre viously established standard curve of TMP through mice skin *in vivo*: A = 0.018∗C + 0.4079, and the drug content in TMP preparation group mice skin was calculated (Table 5). We found that the TMP drug content in the back skin of mice in the T-Lip-AC group was the highest (1.72 ± 0.59 μ g/mL), and the TMP drug content in the T-Lip group was slightly higher than that in the TMP group and T-AC group.

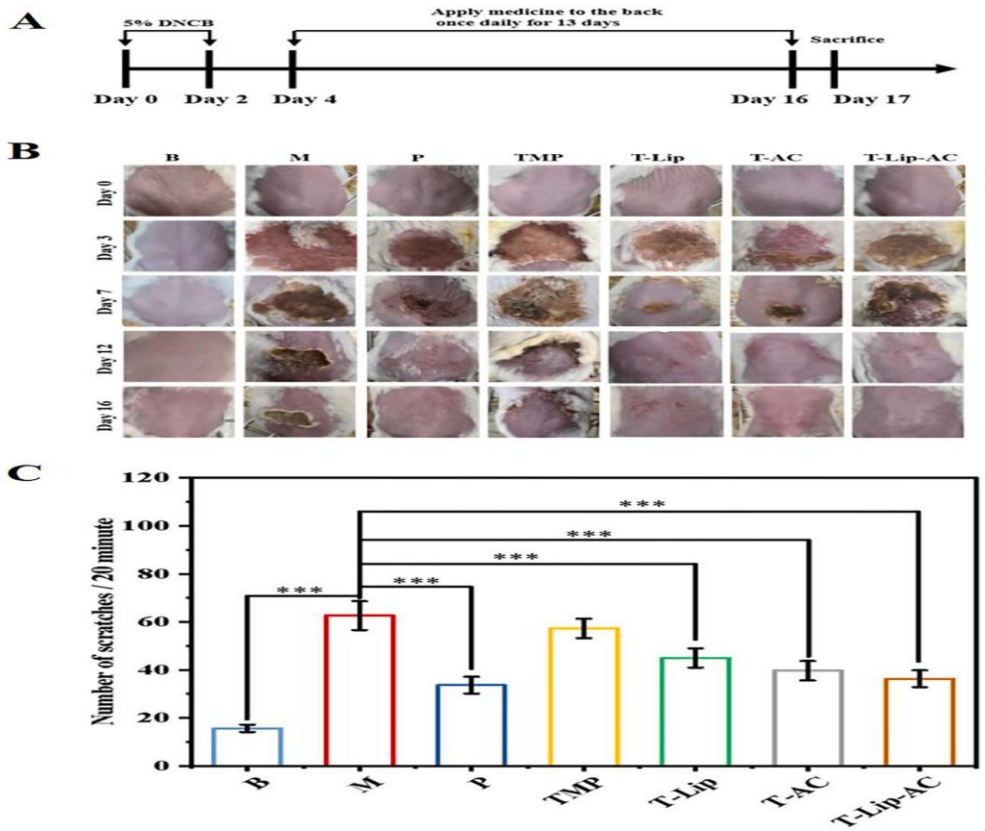

Journal of Chemical Health Risks

www.jchr.org

JCHR (2024) 14(1), 3198-3215 | ISSN:2251-6727

Fig.5. Therapeutic evaluation of T-Lip-AC on DNCB-induced AD mice. (**A**) Schematic diagram of experimental design of AD model; (**B**) The skin condition of mice in each group on day 0, 3, 7, 12 and 16; (**C**) Scratch times of mice in each group/20 minutes. The difference was statistically significant, *** $p<0.001$.

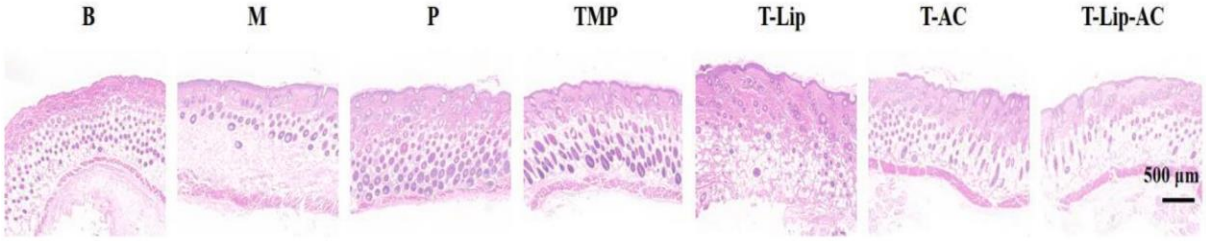

Fig.6. Micro-photos of back skin sections stained with H&E in mice. Scale=500 μm.

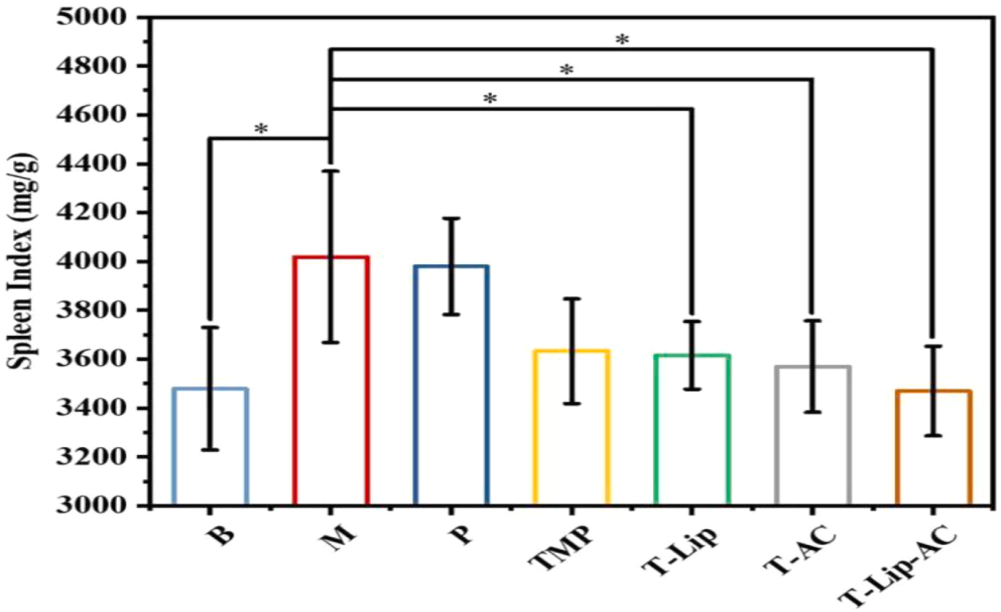

Fig.7. Spleen index of mice. *p <0.05.

4. Discussion

AD is a chronic recurrent inflammatory skin disease characterized by itching, dry, eczema, erythema, and edema, which is widely prevalent worldwide. [24, 25] TMP is an effective and active ingredient in traditional Chinese medicine named Chuanxiong, but it has poor water solubility, rapid metabolism, and low bioavailability. In order to solve this problem, TMP was encapsulated into liposomes to improve its stability and prolong the drug action time. [26] The advantages of using liposomes for skin delivery of drugs have been fully demonstrated. Liposomes as the bio-inspired delivery system have been shown to have the effect of enhancing permeability and delivering a range of drugs with different physical and chemical properties, and can even serve as a warehouse for continuous delivery of drugs requiring local deposition. [27] However, liposomes are unstable and susceptible to damage by factors such as light, acid, and alkalis. [28] This problem could be solved by modifying surface of liposomes with PEC and making hydrogel. For the sake of form a PEC, both polyelectrolytes must have opposite charges. [29] Previous studies have shown that ALG was negatively charged at neutral pH, and most functional groups exist in the form of – COO - . While CS is positively charged at pH=6.0, most functional groups exist in the form of - NH3 +. Under this condition, the carboxyl group of negatively charged ALG can electrostatic interact with the amino group of positively charged CS to form amide bond, which is the main chemical bond in the hydrogel. [30, 31] However, because ALG and CS have opposite charges, PEC formed by two opposite polyelectrolytes cannot exist stably in the solution during blending, so agglomeration precipitation occurs. To this end, we use inorganic salt NaCl as a charge shielding agent to weaken the charge strength of PEC to obtain a stable blend solution. [32]

Journal of Chemical Health Risks

www.jchr.org

JCHR (2024) 14(1), 3198-3215 | ISSN:2251-6727

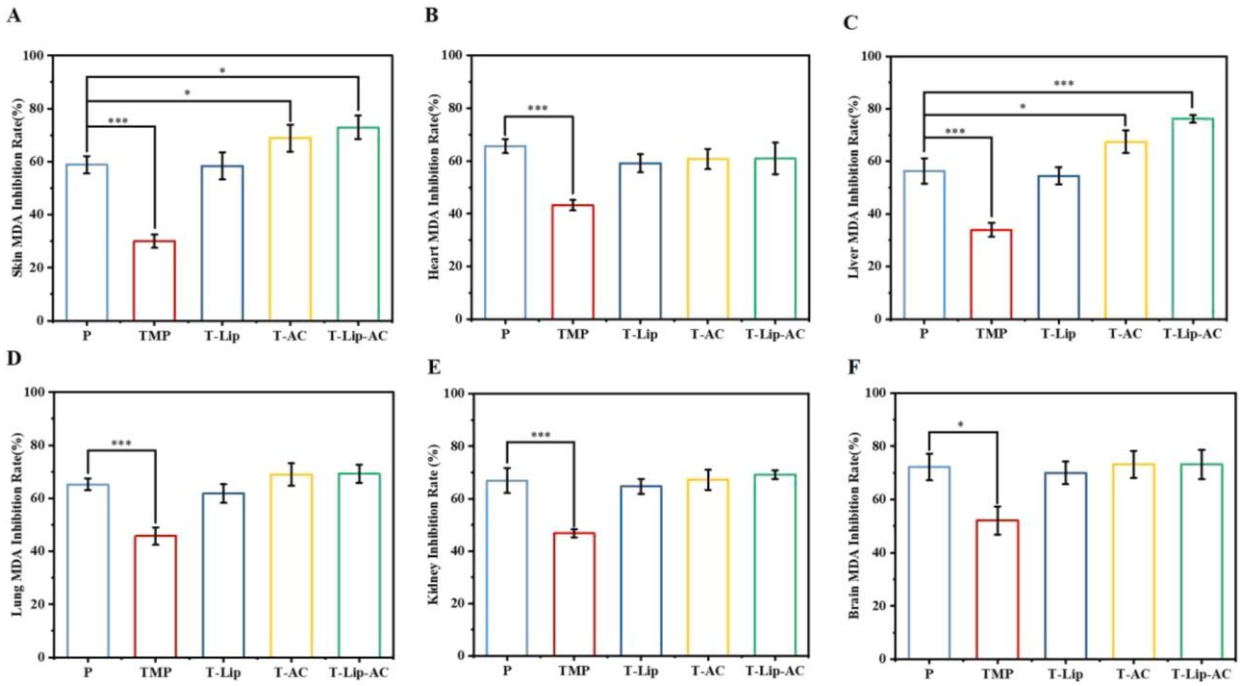

Fig.8. The inhibition rate on MDA in different tissue homogenates. (A) Skin; (B) Heart; (C) Liver; (D) Lung; (E) Kidney; (F) Brain. ***p <0.001; *p <0.05.

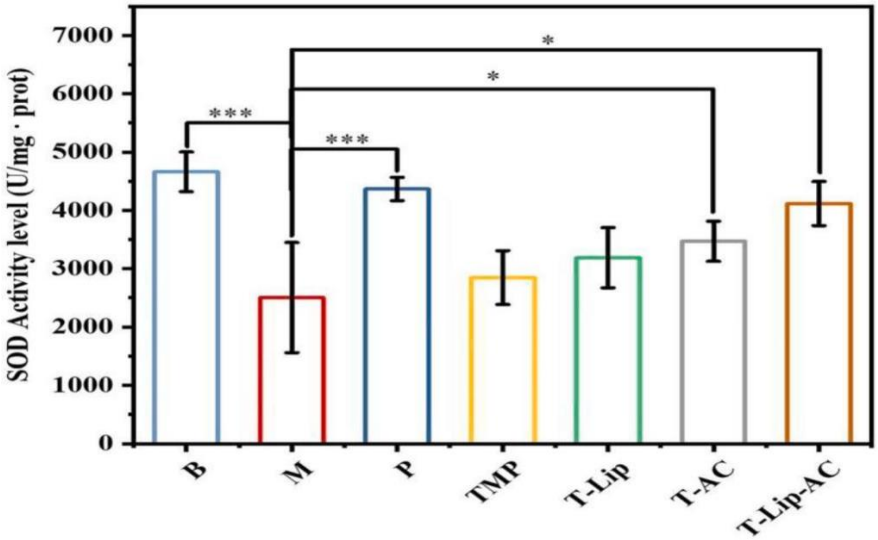

Fig.9. SOD activity level of mice skin. ***p <0.001; *p <0.05.

Table 2. Study on the content of different TMP preparations in the skin of mice with AD-like symptoms.

Group	Drug Concentration (μg/mL)
TMP	1.28 ± 0.37
T-Lip	1.41 ± 0.47
T -AC	1.36 ± 0.41
T-Lip-AC	1.72 ± 0.59

However, when the amount of shielding agent is fixed, the ratio of ALG to CS will affect the transparency of the hydrogel. At the same time, in order to enhance the crosslinking and viscosity of hydrogels, ALG-CS hydrogels must react with covalent or ionic crosslinkers (Ca2+ or Al3+ ions) to produce a stronger cross-linked polyelectrolyte system under acidic/neutral conditions. [33] It is worth noting that at pH values above 6.5, the

Journal of Chemical Health Risks

www.jchr.org

JCHR (2024) 14(1), 3198-3215 | ISSN:2251-6727

number of uncharged amine groups in CS increases, and the probability of repulsion between the – COO - and - NH2 groups also increases. Accordingly, we may observe a phenomenon of increased PEC swelling. Nevertheless, this phenomenon did not be observed in T-AC and T-Lip-AC hydrogels, which may be due to the presence of Ca2+ and its formation of complexes with amino and carboxylic groups, resulting in the formation of resistant PECs in a wide pH range. This result is consistent with the published research results. [34, 35] Besides, it has been reported in relevant literature that when the ALG-CS hydrogel is generated by using Ca2+ as a crosslinking agent, CS does not react with Ca2+, and ALG is responsible for specific binding with Ca2+. [36] And Ca2+ forms a complex with a coordination number of 4 with ALG through hydroxyl and carboxyl groups. [37] The schematic illustration of ALG-CS hydrogels PEC reinforced with Ca2+ and the interactions between polymers are shown in Fig. 10. The characteristic of AD disease skin is the appearance of a dry stratum corneum, which requires effective hydration and diffusion to trigger a drug response to the treatment of AD skin. [38] Consequently, we need to develop a hydrogel with good moisture absorption ability, which can effectively reduce the accumulation of wound exudate and keep the wound in a moderately wet environment. In terms of hygroscopicity experiments, we found that T-Lip-AC hydrogel could provide a wet healing environment for dry wounds to a certain extent, and also absorb moisture for wounds with certain exudates. This feature not only helps to absorb exudates that may interfere with wound healing, but also maintains a wet environment for cell adhesion, migration and proliferation. More importantly, ALG-CS hydrogel has a porous three-dimensional network structure and this hydrogel with three-dimensional porous structure and good hydrophilicity ensure the transport of nutrients and the exchange of biological molecules with internal cells. It is conducive to the reestablishment of the skin barrier and the recovery of epidermal wounds with AD symptoms. [39]

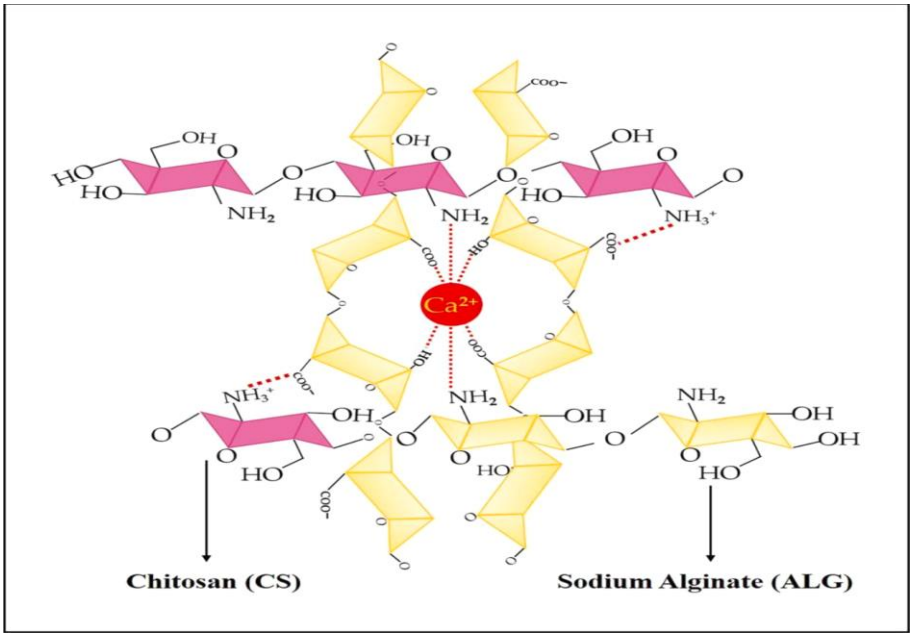

Fig.10. The schematic illustration of ALG-CS hydrogels PEC reinforced with Ca2+ and the interactions between polymers.

In the drug transmembrane release experiment across dialysis membrane (Fig. 3A), we found that except for TMP solution, other TMP preparations showed significant biphasic release behavior. Compared with other preparations, the release rate of T-Lip-AC in the first stage was relatively slow, while the release rate in the later stage was faster. The total duration was 24 h, and the range increased from 1.9 ± 0.07% to 61.07 ± 4.73%. This release behavior was mainly due to T-Lip-AC not only passing through the lipid bilayer, but also through the three-dimensional network structure of ALG-CS. [40] The ultimate maximum release of T-AC in the first stage was due to its rapid release and adsorption onto the surface of ALG-CS, and the three-dimensional network structure of ALG-CS extended the drug release time. The second stage, which extends from 24 h to 96 h, was achieved through a diffusion mechanism and resulted in prolonged drug release due to the slow dissolution and dispersion of the three-dimensional network structure of the lipid core matrix

Journal of Chemical Health Risks

www.jchr.org

JCHR (2024) 14(1), 3198-3215 | ISSN:2251-6727

and ALG-CS. In the drug transdermal release experiment across isolated skin (Fig. 3B), the penetration of TMP from T-Lip-AC hydrogel increased by 1.6 times compared with free TMP solution. In the experiment of detecting the TMP drug content of various preparations in the AD-like mice skin, it was found that the T-Lip-AC group had the highest TMP drug content in the mice back skin (Table 5). Compared with free TMP solution, the improvement of T-Lip-AC hydrogel in skin penetration was mainly due to the lipophilic nature of the skin barrier. Liposome was amphiphilic, and its lipophilicity allowed T-Lip in T-Lip-AC to rapidly penetrate through the stratum corneum to the lower dermis, enter the systemic circulation, enhance the efficacy of drugs in the body. Further, liposomes nanoparticles with sizes smaller than 200 nm have been reported to penetration into the skin and systemic circulation under AD-like conditions.

The T-Lip-AC hydrogel we prepared is spherical, in which the liposomes nanoparticles size is<200 nm. And smaller liposomes nanoparticles (<200 nm) can easily penetrate cellular tissues due to their enhanced permeability and retention effects, improving the efficacy of the drug *in vivo*, which is beneficial for the systemic treatment of AD disease. Besides, CS could be used as a skin penetration enhancer to help liposome nanoparticles penetrate the skin. ALG-CS hydrogel has some similarities with human skin tissue materials so it has good biocompatibility and certain controlled release function. Overall, T-Lip-AC provided TMP with good drug release and enhanced drug transdermal delivery, which might be beneficial for the treatment of AD. Bacterial infections produce large inflammatory factors to attack the wound site, leading to cell damage and inflammation. These factors can seriously affect cell proliferation and wound healing. And AD patients' skin is more susceptible to bacterial infections. [41] Thus, T-Lip-AC hydrogel should have excellent antibacterial ability during the treatment of AD. This study found that T-Lip-AC hydrogel slowed down the formation of bacteria and had antibacterial effect compared with T-Lip without ALG-CS. It has been reported that the protonated amino group of CS can interact with the cell membrane of negatively charged bacteria to generate electrostatic interactions, leading to bacterial permeability, leading to leakage of substances within the bacteria, and ultimately leading to bacterial death. In addition, CS can also affect the expression of bacterial DNA by binding to bacterial nucleic acids. Recently, inflammatory reactions and oxidative stress have been proven to be related to the pathogenesis and progression of AD. ROS is typically defined as a partially reduced oxygen metabolite with strong oxidative capacity. Currently, members of the ROS family that are widely studied and understood include superoxide anion (O2 - ·), hydroxyl radical (OH·), nitrogen containing radical (such as DPPH), H2O2, and hypochlorous acid (HClO). According to reports, inflammatory stimulation could lead to the activation of neutrophils, which in turn can lead to the production of ROS. At low concentrations ROS as a signaling molecule that regulates cell growth, cell adhesion to other cells, differentiation, aging, and apoptosis. However, high concentrations of ROS are harmful to normal human cells because they can oxidize protein and lipid cell components and destroy DNA, leading to an imbalance in the body's redox response and the development of various inflammatory diseases. [42] When the production of oxidants or ROS exceeds the endogenous antioxidant capacity of the human body, oxidative stress occurs. Therefore, oxidative stress can be described as an imbalance between ROS. In addition, some researchers have found that excessive ROS can cause delayed wound repair and healing. Therefore, the ideal hydrogel for treating AD should be able to remove excess ROS and protect cells and tissues from ROS induced damage. TMP has been shown to have strong antioxidant and anti-inflammatory activities. Accordingly, in order to verify the antioxidant effect of TMP on ROS, the scavenging rates of different concentrations of TMP solutions on H2O2 and DPPH free radicals *in vitro* was measured.

For the sake of further determine the antioxidant activity of TMP containing preparations and the impact of excipients on their antioxidant performance. The scavenging ability of TMP solution, T-Lip, T-AC, and T-Lip-AC on free radicals was compared. [43] Our research has confirmed that TMP can effectively reduce ROS production *in vitro*, and the anti-inflammatory and antioxidant effects of TMP were synergistically enhanced due to the antioxidant capacity of CS (Fig. 4). The skin administration of T-Lip-AC hydrogel treated AD-like skin lesions in mice induced by DNCB, and significantly restored the severity of AD scores. In addition, T-Lip-AC hydrogel could alleviate the itching caused by DNCB and improve the spleen index. Histopathological analysis showed that T-Lip-AC hydrogel could inhibit DNCB induced epidermal, dermal thickening and mast cell infiltration. When mice develop AD lesions, inflammatory cells infiltrate the damaged site, secreting inflammatory cytokines and oxidative stress related factors (MDA, SOD, etc.), which were related to lipid peroxidation and could cause secondary injury. Therefore, this experiment further analyzed the antioxidant activity of T-Lip-AC by evaluating the levels of MDA and SOD in the tissues of AD diseased mice. The overall level of MDA in the T-Lip-AC group was lower than that in the group P, and the level of SOD was higher than that in the other TMP preparation

Journal of Chemical Health Risks

www.jchr.org

JCHR (2024) 14(1), 3198-3215 | ISSN:2251-6727

groups, and was the closest to that in the group B after 16 days of injury, (Figs. 8 and 9). Therefore, TMP could alleviate AD by inhibiting oxidative stress and inflammatory reactions. TMP-loaded liposome modifying with ALG-CS could significantly improve the anti-inflammatory and antioxidant activities of TMP. [44]

5. Conclusion

The daily use of therapeutic drugs in AD patients often has adverse reactions, and AD patients are prone to bacterial infections. The adverse reactions of AD treatment drugs and antibiotic resistance make it more difficult to treat such diseases. In this experiment, Liposomes surface was modified with ALG and CS to form a multifunctional hydrogel drug delivery system. The results of experimental data indicated that T-LipAC hydrogel modified with Lip and ALG-CS exhibits stronger anti-inflammatory, antioxidant, and antibacterial activities than TMP, and its transdermal delivery ability was also enhanced. It also had a slowing and controlling effect and the ability to provide a moist healing environment for dry skin. In the animal model of AD, T-Lip-AC hydrogel could significantly reduce AD-like symptoms compared to the TMP group. In addition, treatment with T-Lip-AC could alleviate oxidative stress and increase SOD activity in AD animals. In conclusion, this study prepared a multifunctional hydrogel drug delivery system to treat AD symptoms.

Declaration of competing interest

The author declares no conflict of interest, financial or otherwise.

Acknowledgements

This research did not receive any specific grant from funding agencies in the public, commercial, or not-for-profit sectors. The authors are helpful to the National Institute of Technology (NIT), Rourkela, Odisha, India for providing all required facilities. The authors would also like to thank to Columbia Institute of Pharmacy, Raipur, Chhattisgarh, India for providing laboratory animal facilities.

References

1. Abd El-Hack, M.E., El-Saadony, M.T., Shafi, M.E., Zabermawi, N.M., Arif, M., Batiha, G. E., Khafaga, A.F., Abd El-Hakim, Y.M., Al-Sagheer, A.A., 2020. Antimicrobial and antioxidant properties of chitosan and its derivatives and their applications: a review. Int. J. Biol. Macromol. 164, 2726–2744.
2. Albanesi, C., 2010. Keratinocytes in allergic skin diseases. Curr. Opin. Allergy Clin. Immunol. 10, 452–456.
3. Berger, J., Reist, M., Mayer, J.M., Felt, O., Gurny, R., 2004. Structure and interactions in chitosan hydrogels formed by complexation or aggregation for biomedical applications. Eur. J. Pharm. Biopharm. 57, 35–52.
4. Birben, E., Sahiner, U.M., Sackesen, C., Erzurum, S., Kalayci, O., 2012. Oxidative stress and antioxidant defense. World Allergy Organ. J. 5, 9–19.
5. Cannava, C., De Gaetano, F., Stancanelli, R., Venuti, V., Paladini, G., Caridi, F., Ghica, C., Crupi, V., Majolino, D., Ferlazzo, G., Tommasini, S., Ventura, C.A., 2022. Chitosanhyaluronan nanoparticles for vinblastine sulfate delivery: characterization and internalization studies on K-562 cells. Pharmaceutics 14.
6. Dhaliwal, J., Dhaliwal, N., Akhtar, A., Kuhad, A., Chopra, K., 2022. Tetramethylpyrazine attenuates cognitive impairment via suppressing oxidative stress, neuroinflammation, and apoptosis in type 2 diabetic rats. Neurochem. Res. 47, 2431–2444.
7. Elzoghby, A.O., Samy, W.M., Elgindy, N.A., 2012. Albumin-based nanoparticles as potential controlled release drug delivery systems. J. Control Release 157, 168–182.
8. Emmanuel, B.D., Abu-Thabit, N.Y., Ngwuluka, N.C., 2018. Stimuli responsive polymeric nanocarriers for drug delivery applications. In: Woodhead Publishing Series in Biomaterials, 1. Woodhead Publishing, pp. 267–287.
9. Feng, J., Li, F., Zhao, Y., Feng, Y., Abe, Y., 2009. Brain pharmacokinetics of tetramethylpyrazine after intranasal and intravenous administration in awake rats. Int. J. Pharm. 375, 55–60.
10. Frohm, M., Gunne, H., Bergman, A.C., Agerberth, B., Bergman, T., Boman, A., Liden, S., Jornvall, H., Boman, H.G., 1996. Biochemical and antibacterial analysis of human wound and blister fluid. J. Biochem. 237, 86–92.
11. Gierszewska, M., Ostrowska-Czubenko, J., Chrzanowska, E., 2018. pH-responsive chitosan/alginate polyelectrolyte complex membranes reinforced by tripolyphosphate. Eur. Polym. J. 101, 282–290.
12. Gonzalez-Rodriguez, M.L., Rabasco, A.M., 2011. Charged liposomes as carriers to enhance the permeation through the skin. Expert Opin. Drug Deliv. 8, 857–871.
13. Holsaeter, A.M., Wizgird, K., Karlsen, I., Hemmingsen, J.F., Brandl, M., SkalkoBasnet, N., 2022. How docetaxel entrapment, vesicle size, zeta potential and stability change with liposome composition-A formulation screening study. Eur. J. Pharm. Sci. 177, 106267.
14. Homey, B., Steinhoff, M., Ruzicka, T., Leung, D.Y., 2006. Cytokines and chemokines orchestrate

Journal of Chemical Health Risks

www.jchr.org

JCHR (2024) 14(1), 3198-3215 | ISSN:2251-6727

atopic skin inflammation. J. Allergy Clin. Immunol. 118, 178–189.

15. Javia, A., Misra, A., Thakkar, H., 2022. Liposomes encapsulating novel antimicrobial peptide Omiganan: characterization and its pharmacodynamic evaluation in atopic dermatitis and psoriasis mice model. Int. J. 624.
16. Jiang, R., Xu, J., Zhang, Y., Liu, J., Wang, Y., Chen, M., Chen, X., Yin, M., 2022. Ligustrazine alleviates psoriasis-like inflammation through inhibiting TRAF6/cJUN/NFkappaB signaling pathway in keratinocyte. Biomed. Pharmacother. 150, 113010.
17. Kothale, D., Verma, U., Dewangan, N., Jana, P., Jain, A., Jain, D., 2020. Alginate as promising natural polymer for pharmaceutical, food, and biomedical applications. Curr Drug Deliv. 17, 755–775.
18. Kubota, K., Saiwai, H., Kumamaru, H., Maeda, T., Ohkawa, Y., Aratani, Y., Nagano, T., Iwamoto, Y., Okada, S., 2012. Myeloperoxidase exacerbates secondary injury by generating highly reactive oxygen species and mediating neutrophil recruitment in experimental spinal cord injury. Spine 37, 1363–1369.
19. Kuhn, P.T., Rozenbaum, R.T., Perrels, E., Sharma, P.K., Van Rijn, P., 2017. Antimicrobial biopolymer hydrogel scaffolds for stem cell encapsulation. Polymers (Basel) 9.
20. Lee, Y.I., Lee, S.G., Kim, J., Choi, S., Jung, I., Lee, J.H., 2021. Proteoglycan combined with hyaluronic acid and hydrolyzed collagen restores the skin barrier in mild atopic dermatitis and dry, eczema-prone skin: a pilot study. Int. J. Mol. Sci. 22.
21. Li, J., Gong, X., 2022. Tetramethylpyrazine: an active ingredient of chinese herbal medicine with therapeutic potential in acute kidney injury and renal fibrosis. Front. Pharmacol. 13, 820071.
22. Li, J., Zhuang, S., 2020. Antibacterial activity of chitosan and its derivatives and their interaction mechanism with bacteria: current state and perspectives. Eur. Polym. J. 138.
23. Liu, T., Feng, Z., Li, Z., Lin, Z., Chen, L., Li, B., Chen, Z., Wu, Z., Zeng, J., Zhang, J., Hong, J., Xia, H.,Liu, X., Testa, B., Fahr, A., 2011. Lipophilicity and its relationship with passive drug permeation. Pharm. Res. 28, 962–977.
24. Ma, Y., Cong, Z., Gao, P., Wang, Y., 2023. Nanosuspensions technology as a master key for nature products drug delivery and *in vivo* fate. Eur. J. Pharm. Sci. 185, 106425.
25. Mengoni, T., Adrian, M., Pereira, S., Santos-Carballal, B., Kaiser, M., Goycoolea, F.M., 2017. A chitosan-based liposome formulation enhances the in vitro wound healing efficacy of substance P neuropeptide. Pharmaceutics 9.
26. Mittal, M., Siddiqui, M.R., Tran, K., Reddy, S.P., Malik, A.B., 2014. Reactive oxygen species in inflammation and tissue injury. Antioxid. Redox. Signal. 20, 1126–1167.
27. Nagarwal, R.C., Kumar, R., Pandit, J.K., 2012. Chitosan coated sodium alginate-chitosan nanoparticles loaded with 5-FU for ocular delivery: *in vitro* characterization and *in-vivo* study in rabbit eye. Eur. J. Pharm. Sci. 47, 678–685.
28. Nogueira, E., Gomes, A.C., Preto, A., Cavaco-Paulo, A., 2015. Design of liposomal formulations for cell targeting. Colloids Surf. B Biointerfaces 136, 514–526.
29. Ong, P.Y., Leung, D.Y., 2016. Bacterial and viral infections in atopic dermatitis: a comprehensive review. Clin. Rev. Allergy 51, 329–337.
30. Pan, W., Qi, X., Xiang, Y., You, S., Cai, E., Gao, T., Tong, X., Hu, R., Shen, J., Deng, H., 2022. Facile formation of injectable quaternized chitosan/tannic acid hydrogels with antibacterial and ROS scavenging capabilities for diabetic wound healing. Int. J. Biol. Macromol. 195, 190–197.
31. Pathak, J., Priyadarshini, E., Rawat, K., Bohidar, H.B., 2017. Complex coacervation in charge complementary biopolymers: electrostatic *versus* surface patch binding. Adv. Colloid Interface Sci. 250, 40–53.
32. Rowland, R.N., Woodley, J.F., 1980. The stability of liposomes *in vitro* to pH, bile salts and pancreatic lipase. Biochim. Biophys. Acta 620, 400–409.
33. Schafer, M., Werner, S., 2008. Oxidative stress in normal and impaired wound repair. Pharmacol. Res. 58, 165–171.
34. Seykora, J., Dentchev, T., Margolis, D.J., 2015. Filaggrin-2 barrier protein inversely varies with skin inflammation. Exp. Dermatol. 24, 720–722.
35. Shetty, K., Sherje, A.P., 2021. Nano intervention in topical delivery of corticosteroid for psoriasis and atopic dermatitis-a systematic review. J. Mater. Sci. Mater. Med. 32, 88.
36. Ta, Q., Ting, J., Harwood, S., Browning, N., Simm, A., Ross, K., Olier, I., Al-Kassas, R., 2021. Chitosan nanoparticles for enhancing drugs and cosmetic components penetration through the skin. Eur. J. Pharm. Sci. 160, 105765.
37. Thannickal, V.J., Fanburg, B.L., 2000. Reactive oxygen species in cell signaling. Am. J. Physiol. Lung Cell. Mol. Physiol. 279, L1005–L1028.
38. Thomas, S., Hay, P., 1995. Fluid handling properties of hydrogel dressings. Ostomy Wound Manage. 41, 54–56, 58-59.
39. Wang, S., Gao, Z., Liu, L., Li, M., Zuo, A., Guo, J., 2022b. Preparation, *in vitro* and *in vivo* evaluation of chitosan-sodium alginate-ethyl cellulose

polyelectrolyte film as a novel buccal mucosal delivery vehicle. Eur. J. Pharm. Sci. 168, 106085.

40. Wang, Y., Yue, Y., Jia, R., Liu, X., Cheng, Z., Cheng, Y., Xu, Y., Xie, Z., Xia, H., 2023. Design and evaluation of paeonol-loaded liposomes in thermoreversible gels for atopic dermatitis. Gels 9.
41. Xia, H., Cheng, Z., Cheng, Y., Xu, Y., 2016. Investigating the passage of tetramethylpyrazine-loaded liposomes across blood-brain barrier models *in vitro* and ex vivo. Mater. Sci. Eng. C Mater. Biol. Appl. 69, 1010–1017.
42. Yu, K., Chen, Z., Pan, X., Yang, Y., Tian, S., Zhang, J., Ge, J., Ambati, B., Zhuang, J., 2012. Tetramethylpyrazine-mediated suppression of C6 gliomas involves inhibition of chemokine receptor CXCR4 expression. Oncol. Rep. 28, 955–960.
43. Zhang, Q., Yang, X., Wu, Y., Liu, C., Xia, H., Cheng, X., Cheng, Y., Xia, Y., Wang, Y., 2022a. In vitro evaluation of Kaempferol-loaded hydrogel as pH-sensitive drug delivery systems. Polymers (Basel) 14.
44. Zhang, Y., Ma, C., He, L., Liao, L., Guo, C., Wang, C., Gong, L., Zhou, H., Fu, K., Peng, C., Li, Y., 2022b. Tetramethylpyrazine protects endothelial injury and antithrombosis via antioxidant and antiapoptosis in HUVECs and Zebrafish. Oxid. Med. Cell Longev. 2022, 2232365.